Le Boson H, Séminaire Poincaré XIX (2014) 47 – 73 Séminaire Poincaré

Discovery and Measurements of the H Boson with ATLAS and CMS Experiments at the LHC

Yves Sirois*
LLR École Polytechnique, CNRS-IN2P3
E:mail: yves.sirois@in2p3.fr

Abstract. The discovery of a new boson with a mass around 125 GeV has been established in July 2012 by the ATLAS and CMS experiments at the LHC collider. More than twice as much data was collected by the end of 2012. The analysis of the full data sample, collected with pp collisions at 7 and 8 TeV in 2011 and 2012, has now allowed for considerable progress in understanding the nature of the new boson. The new boson is found to be a Higgs boson, with properties as expected for the scalar boson H resulting from the Brout-Englert-Higgs mechanism responsible for electroweak symmetry breaking in the standard model. A review of the latest ATLAS and CMS results on the H boson is presented here.

1 Introduction: the Standard Model and the Higgs Boson

Over the past four decades, the standard model (SM) of particle physics has provided a remarkably accurate description of numerous results from accelerator and non-accelerator based experiments. Yet, until very recently, the question of how the W and Z gauge bosons acquire mass remained an opened question. This question could have jeopardized the validity of the theory at higher energies or, equivalently, at smaller distance scales. Understanding the origin of the electroweak symmetry breaking (EWSB), how the W and Z bosons acquire mass whilst the photon remains massless, has been set as one of the most important objectives of the Large Hadron collider (LHC) physics program at the birth of the project more than twenty years ago. The SM remained an unchallenged [1] but incomplete theory for the interactions of particles until the Large Hadron Collider (LHC) finally provided its first high energy proton-proton collisions at 7 TeV in 2010. The discovery of a new boson at a mass of about 125 GeV by the ATLAS [2] and CMS [3, 4] experiments in 2012, and

*This review evolved from a review in preparation for the "Comptes Rendues de l'Académie des Sciences" and written in collaboration with, Rosy Nicolaidou, IRFU, CEA-Saclay.

the confirmation with additional data that the boson behaves like a Higgs boson, have now considerably changed the landscape.

The SM comprises matter fields, the quarks and leptons as the building blocks of matter, and describes their interactions through the exchange of force carriers: the photon for electromagnetic interactions, the W and Z gauge bosons for weak interactions, and the gluons for strong interactions. The electromagnetic and weak interactions are partially unified in the Glashow-Weinberg-Salam electroweak theory [5, 6, 7]. The gauge bosons are a direct consequence of the underlying gauge symmetries. It is sufficient to postulate the invariance under SU(2) $\times$ U(1) gauge symmetry in the electroweak sector to see emerging as a necessity the existence of the photon, for the electromagnetic interaction, and the W and Z bosons, for the weak interactions. The gauge symmetries are the essential pillars of the theory and thus must be preserved. This is only possible if the gauge bosons remain massless in the fundamental theory. Besides the question of the origin of the mass of vector bosons, the very existence of these massive bosons was threatening the theory at the TeV scale. In contrast to quantum electrodynamics where a renormalizable theory is obtained by injecting the masses and charges measured at a given scale by hand, no such trick is possible for the weak interaction while preserving the gauge symmetries. The massive vector bosons lead to violation of unitarity for calculations at the TeV scale, unless something else is added. The SM with the gauge bosons and matter fields is incomplete. Additional structure is needed.

Since the advent of the electroweak theory, the Brout-Englert-Higgs (BEH) mechanism [8, 9, 10, 11, 12, 13] had been adopted as a solution to both the EWSB and the unitarization of the theory. In this mechanism, the introduction of a complex scalar doublet field with self interactions allows for a spontaneous EWSB. This leads to the generation of the W and Z masses, the weak boson acquiring longitudinal degrees of freedom, and to the prediction of the existence of one physical Higgs boson (H). The fundamental fermions also acquire mass through Yukawa interactions with the scalar field when propagating in the physical vacuum: the left- and right-handed chiralities become coupled. The mass m_{H} of the Higgs boson in the SM is not predicted by the theory, but general considerations [14, 15, 16, 17] on the finite self-coupling of the Higgs field, the stability of the vacuum, and unitarization bounds suggest that it should be smaller than about 1 TeV. The existence of a scalar boson is sufficient to allow for an exact unitarization of the theory. But saving the theory has a cost: the arbitrariness m_{H} (and of the self-couplings) and the fact that the Higgs boson is not a gauge boson. Thus the mass m_{H} is not protected by any symmetry of the theory. The mass is sensitive to any new scale beyond the SM which could contribute in quantum fluctuations. The theory would have to be fine tuned to maintain m_{H} at the weak scale.

With these considerations in mind, the scene is set to describe the search, the discovery, and the measurements of the Higgs boson at the LHC. This review is organized as follows. First, we fbriefly describe the ATLAS and CMS experiments in section 2. We then focus on the H boson and remind about the relevant phenomenology aspects in section 3. In section 4, we recollect the adventure of the search for the Higgs boson at the LEP e^+e^- collider, the Tevatron $p\bar{p}$ colllider, and the LHC pp collider including data collected at $\sqrt{s} = 7\,\mathrm{TeV}$ in 2011. The additional data collected at the LHC at $\sqrt{s} = 8\,\mathrm{TeV}$ lead, in July 2012, to the discovery of the new boson via di-boson channels as reminded in section 4. We then turn in section 5 to the

measurement of the properties of the Higgs boson using all available LHC data from run I, starting with the high resolution channels and the measurement of the Higgs boson mass, then with constraints on the resonance width, tests and constraints on the spin-parity state, comparisons of the signal rates with SM expectation in various production and decay modes, and finally the coupling constraints and compatibility with SM expectation. We conclude in section 6 with some elements of prospects for the future data taking at the LHC.

2 The ATLAS and CMS experiments

The ATLAS ("A Toroidal LHC Apparatus") [18] and CMS ("Compact Muon Solenoid") [19] detectors are multi-purpose devices with a cylindrical geometry, and forward-backward symmetry along the beam line. Both experiments have been designed to allow for a good measurement of leptons from low to very high momenta, offer sufficient transverse or longitudinal granularity to provide a high discrimination of isolated leptons against QCD instrumental background, and provide a nearly 4π solid angle coverage for the measurement of hadronic jets and transverse energy flow. Above all other considerations, the detailed design of the experiments follows from the choice of the main magnets. The CMS experiment has chosen a solenoid which allows for a compact detector. The solenoid provides field lines parallel to the Z (beam) axis so that charged particles trajectories bend in the transverse plane. The excellent momentum resolution required for TeV muons is made possible via a very high magnetic field and a fine grained tracker. The ATLAS experiment has chosen a toroid which imposes a very large volume. The toroid provides field lines which are circles centered on the Z axis, so that muons bend in a plane defined by the beam axis and the muon position. This provides excellent stand alone momentum resolution for TeV muons, but an internal solenoid is needed for the purpose of vertex reconstruction and additional momentum measurements with a fine grained tracker. The experiments were ready to take data in 2008, after about 15 years of research and developments, design and construction

Three-dimensional representations of the ATLAS and CMS detectors are shown Fig. 1. The ATLAS layout comprises a thin superconducting solenoid surrounding inner tracking detectors and three large superconducting toroids supporting a large muon tracker. The inner detectors consist of a silicon pixel device, a silicon microstrip device and a transition radiation tracker, all immersed in the 2 Tesla field from the solenoid. High-granularity liquid-argon (LAr) electromagnetic sampling calorimeters cover the pseudorapidity region $|\eta| < 3.2$. An iron-scintillator tile calorimeter provides coverage over $|\eta| < 1.7$. The end-cap and forward regions, spanning $1.5 < |\eta| < 4.9$, are instrumented with LAr calorimetry for both electromagnetic and hadronic measurements. The muon spectrometer covering $|\eta| < 2.7$ relies on the magnetic deflection of muons tracks in the air-core toroid magnets, instrumented with separate trigger and high-precision tracking chambers The CMS layout comprises a superconducting solenoid of 6 m internal diameter, providing a uniform magnetic field of 3.8 T. The bore of the solenoid is instrumented with various particle detection systems. The inner tracking system is composed of a pixel detector with three barrel layers at radii between 4.4 and 10.2 cm and a silicon strip tracker with 10 barrel detection layers extending outwards to a radius of 1.1m. Each

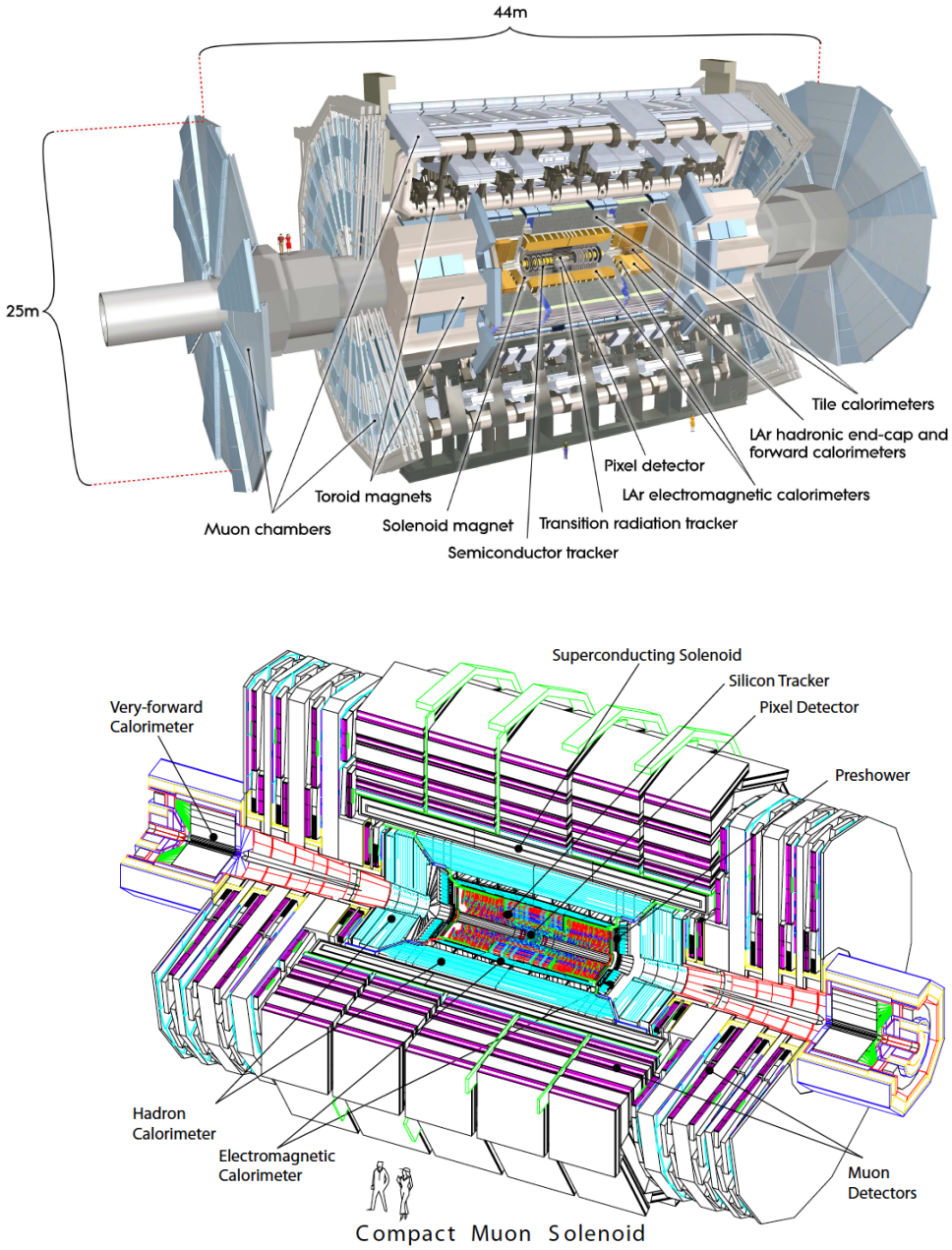

Figure 1: Cut-away three-dimensional view of the ATLAS (top) and CMS (bottom) detectors. The instruments occupy volumes with cylindrical shapes, with dimensions for ATLAS of 44 m in length, 25 m in diameter and a weight of $\sim$ 7000 tons, for CMS of 21.6 m in length, 14.6 m in diameter, and 12500 tons.

system is completed by two end caps, extending the acceptance up to $|\eta| < 2.5$. A lead tungstate crystal electromagnetic calorimeter with fine transverse $(\Delta\eta, \Delta\phi)$ granularity and a brass-scintillator hadronic calorimeter surround the tracking volume and cover the region $|\eta| < 3$. The steel return yoke outside the solenoid is in turn instrumented with gas detectors which are used to identify muons in the

range $|\eta| < 2.4$. The barrel region is covered by drift tubes and the end-cap region by cathode strip chambers. A calorimeter made of steel absorber and quartz fiber extends to coverage in forward regions up to $|\eta| < 5.0$.

Both experiments have profited from many months of training and analysis with cosmic data in 2008 and 2009, before the arrival of the first stable LHC collisions. The first LHC collisions were produced at a proton-proton $\sqrt{s} = 900\,\text{GeV}$ during "pilot" runs and then, after a few weeks, at a record $\sqrt{s} = 2.36\,\text{TeV}$. The data collected by the two large experiments, ATLAS and CMS during these early runs were essentially used to finalize the commissioning of the detectors and the analysis tools, and to validate the computing and data distribution models. In December 2009, the level of readiness of the experiments was such, that first physics results could be produced, in some cases within days or weeks. The first public results concerned basic QCD background properties such as the measurement of the underlying event activity, track multiplicity and transverse momentum flow measurements, or for instance the observation of diffraction in proton-proton collisions. After a short technical stop, the LHC operations have resumed in early spring 2010 at $\sqrt{s} = 7\,\text{TeV}$, the highest energy compatible with a secured and stable functioning of the collider. In the following, we concentrate on results obtained at the LHC during the so-called "run 1" in 2011 and 2012, with pp collisions at $\sqrt{s} = 7$ and $8\,\text{TeV}$.

3 Phenomenology at the LHC

3.1 Production and decay modes

In pp collisions, the Higgs boson is produced dominantly by a gluon fusion (ggH) process involving a virtual top (or bottom) quark loop. The other main production modes are the vector boson fusion (VBF), the "Higgstrahlung" (VH with V=W or Z), and the associated production ($t\bar{t}\,$H). The production modes are illustrated in the Fig. 2. The total production cross sections for a SM Higgs [20] boson at the

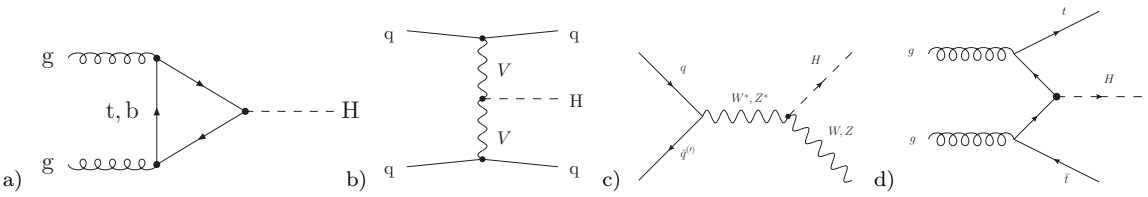

Figure 2: Examples of leading order Feynman diagrams contribution to the production of the SM Higgs boson in hadronic collisions; (a) gluon-gluon fusion $gg \to$ H through b- and t-quark fermion loops; (b) vector boson fusion WWH or ZZH; (c) Higgs-strahlung WH or ZH; (d) associated production of a Higgs boson and a $t\bar{t}$ pair.

LHC are shown as a function of m_{H} in Fig. 3 (left). For $m_{\text{H}} = 125\,\text{GeV}$, the total production cross section is of about 22 pb at a centre of mass of $\sqrt{s} = 8\,\text{TeV}$ (about 17 pb at $\sqrt{s} = 7\,\text{TeV}$). The Higgs boson is thus expected to be copiously produced at the LHC. For this mass, about 87% of the Higgs bosons are produced via ggH, 7.1% via VBF, 4.9% via VH, and 0.6 % via $t\bar{t}\,$H. It is worth mentioning that a huge effort to provide the theoretical cross section calculations at next-to-next-to-leading

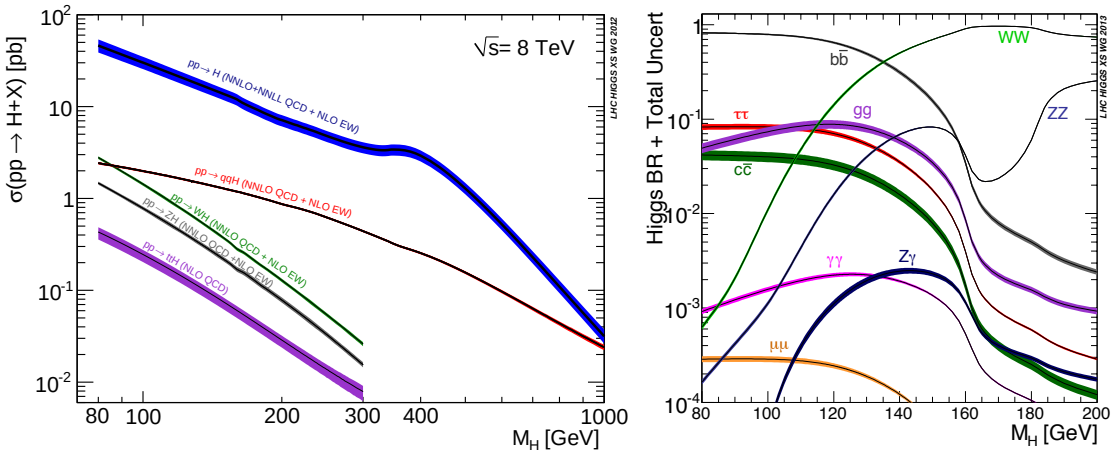

Figure 3: (*left*) Standard model Higgs boson production cross sections at $\sqrt{s} = 8\,\text{TeV}$. (*right*) Branching ratio (BR) for the standard model Higgs boson. The plots are courtesy of Ref. [20] and reproduced here for convenience.

order (NNLO) level has been done the past years and this effort continues with increased interest.

The decay branching ratios for a SM Higgs boson [20] are shown in Fig. 3 (right). The WW di-boson decay dominates at high masses, for $m_{\text{H}} > 135\,\text{GeV}$. The WW and ZZ di-boson decays are the sole relevant modes for $m_{\text{H}} > 2 \times m_{\text{W}}$. At low mass, the $b\bar{b}$ and $\tau\bar{\tau}$ decays are the dominating modes. The intermediate mass range of $115 < m_{\text{H}} < 135\,\text{GeV}$ offers the maximal sharing of the total decay width between the various decay channels. The decays in $c\bar{c}$ or gluon pairs are essentially unobservable as they are overwhelmingly swamped by di-jet QCD background. For $m_{\text{H}} = 125\,\text{GeV}$, this takes away from observation about 11.5% of the Higgs bosons. For this mass, the di-fermions represent about 64.0% of the decays; that is 58 % of the Higgs bosons decaying in $b\bar{b}$ pairs, and about 6 % in $\tau\bar{\tau}$ pairs. About 24.4% branching fraction is left for the di-bosons; that is 0.228% for $\gamma\gamma$, 21.5% for WW, and 2.64% for ZZ decays. Two high mass resolution decay modes offer the best discovery potential in the intermediate masse range, the $\text{H} \to \gamma\gamma$, and the decay chain $\text{H} \to \text{ZZ}^* \to 4\ell$ (in short $\text{H} \to 4\ell$) with at least one Z boson off-mass shell and $\ell = e, \mu$. Real photons being massless, the $\text{H} \to \gamma\gamma$ decay proceeds at leading order via a fermion (mostly top quark) or boson (W) virtual loop as illustrated in Fig. 4. The W loop contribution to the decay dominates. The W loop and top quark loop

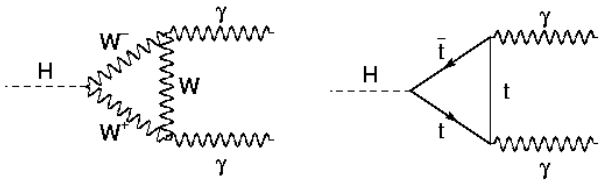

Figure 4: Examples of leading order Feynman diagrams contribution to the decay of the SM Higgs boson in two photons.

contributions interfere destructively such that the W+top contributions are overall about 23% smaller than the W contribution alone. While the $H \to \gamma\gamma$ decay is a rare decay mode, with its branching fraction of about 2×10^{-3} for $m_H = 125\,\text{GeV}$, the $H \to 4\ell$ decay is even rarer, with a branching fraction of about 1.2×10^{-4} for $m_H = 125\,\text{GeV}$ when considering $4\ell = 4e, 4\mu$ and $2e2\mu$ final states.

3.2 Overview of the analysis channels

For a given Higgs boson mass hypothesis, the sensitivity for the search and measurements in a given final state depends on the product of the production cross section and branching fraction to that final state, the reconstructed mass resolution, the signal selection efficiency, and the level of SM backgrounds in the relevant Higgs boson signal phase space. A list of production and decay channels explored during run I at the LHC by the ATLAS and CMS experiments, as well as an indication of the reconstructed Higgs boson mass resolution achievable in each final state, are given in Table 1. In each experiment, the pp collision events are first selected to create

Table 1: Production and decay channels explored during run I at the LHC. The channels labelled "$\star\star\star$" are observed by the ATLAS and/or CMS experiments and used for the determination of the Higgs boson mass and spin-parity state. Evidence is obtained for the channels labelled "$\star\star$". A sensitivity approaching the SM expectation is obtained for those labelled "$\star$". All above channels enter the ATLAS and/or CMS global combinations to constrain the Higgs boson couplings. The sensitivity is found well below SM expectation for the channels labelled with a "$\circ$". The channels labelled "- -" are out of reach.

Decay channel	$\Delta M/M$	Production Modes			
	(sub-channel)	ggH	VBF	VH	$t\bar{t}$H
$H\to\gamma\gamma$	1-2%	$\star\star\star$	$\star\star$	$\star$	$\circ$
$H\to ZZ^*$	1-2% (4ℓ)	$\star\star\star$	$\star$	$\circ$	$\circ$
$H\to W^+W^-$	20-30% ($2\ell2\nu$)	$\star\star\star$	$\star\star$	$\star$	$\circ$
$H\to b\bar{b}$	10-15%	- -	$\circ$	$\star\star$	$\star$
$H\to \tau^+\tau^-$	15-20%	$\star$	$\star\star$	$\star$	$\circ$
$H\to Z\,\gamma$	1-2 %	$\star$	$\circ$	- -	- -
$H\to \mu^+\mu^-$	¡ 1%	$\circ$	$\circ$	- -	- -

partitions corresponding to mutually exclusive channels. These channels are then studied in stand-alone analyses, or re-combined via a statistical method to improve the measurements of the Higgs boson properties.

The $H \to WW^{(*)} \to 2\ell2\nu$, channel covers a wide mass range, but suffers from the lack of mass resolution due to the escaping neutrinos. This was the main channel used at the LHC for early searches of the Higgs boson, with a best sensitivity for a mass hypothesis around $m_H \simeq 2 \times m_W$. This was complemented for the search at higher mass by the $H \to ZZ$ channels (4ℓ and $2\ell2\nu$), and at lower mass by a combination of the $H \to ZZ^* \to 4\ell$ and $H \to \gamma\gamma$ channels. The $H \to \gamma\gamma$ and the $H \to ZZ^* \to 4\ell$ channels provide a distinctive signal with a narrow peak over a smooth background. Evidence for a signal for a mass around 125 GeV in each of these channels, for both experiments, lead to the announcement of a discovery in 2012. The di-boson channels in the $\gamma\gamma$, 4ℓ, and $2\ell2\nu$ final states are the main channels that brought a significant contribution in the statistical combination contemporary

to the discovery. The early searches at the LHC and the discovery of the new boson are discussed further in section 4.

For a Higgs boson mass of about 125 GeV, all five main channels listed first in table 1, namely the di-boson channels $H \to \gamma\gamma$, $H \to ZZ^*$, and $H \to WW^*$, and the fermionic channels $H \to bb$ and $H \to \tau\tau$, can be studied at the LHC using the full run I data.

The $H \to 4\ell$ and $H \to \gamma\gamma$ channels play here again a special rôle as they provide an excellent mass resolution for the reconstructed di-photon and four-lepton final states, respectively. These channels and the Higgs boson mass measurement as well as direct constraints on the width of the resonance will be discussed in more details in section 5.1. With a natural width of the Higgs boson expected to be in the MeV range for $m_H \simeq 125\,\text{GeV}$, and a measurement mass resolution in the GeV range, the direct measurement allows at best to conclude that the observations are consistent with a single narrow resonance. Much more stringent constraints can be obtained in an indirect manner, combining the $H \to 4\ell$ measurements at the 125 GeV resonance, corresponding to the production of a Higgs boson on mass-shell, with measurements at high mass corresponding to the exchange of a Higgs boson off mass-shell. Stringent constraints obtained on the Higgs boson intrinsic width in such a manner will be discussed in section 5.3.

The coupling of the Higgs boson to fermions is best established directly by using the $H \to b\bar{b}$ and $H \to \tau^+\tau^-$ channels. Both channels suffer from large backgrounds and have a poor mass resolution, especially for Higgs bosons produced at low transverse momenta (P_T). For the $H \to b\bar{b}$ decay channel, a sensitivity to the signal can be enhanced by targeting the VH production mode, with V = W or Z, and with subsequent W or Z leptonic decays. For the $H \to \tau\tau$ channel, a sensitivity to the signal can be obtained by considering a combination of events with high reconstructed P_T of the Higgs boson, and events targeting the VBF production of the Higgs boson. The direct coupling to fermions and the question of flavour universality will be discussed in section 5.4.

The measurements in all five main channels in the low mass range ($110 < H < 150\,\text{GeV}$) can be combined to extract signal rates to be compared with SM expectations, and constraints on the Higgs boson couplings. These combined results are discussed in section 5.5.

4 The Search and the Discovery

Direct and model independent searches of the Higgs boson at the LEP e^+e^- collider led to a lower bound on its mass of 114.4 GeV [21] at 95% confidence level (CL). Following the shutdown of the LEP collider in 2000, the direct search for the Higgs boson continued at Fermilab's Tevatron $p\bar{p}$ collider. The $H \to WW \to 2\ell 2\nu$ was the main channel used for early searches at the Tevatron, with background processes from non-resonant WW production and from top-quark production, including $t\bar{t}$ pairs and single-top-quark (mainly tW). With up to $7.1\,\text{fb}^{-1}$ and $8.2\,\text{fb}^{-1}$ of data from the CDF and D0 experiments respectively, the Tevatron combination [22] in 2011 excluded the range $158 - 173\,\text{GeV}$. At this time, the LHC experiments were ready to take over.

Meanwhile, indirect constraints had been derived by exploiting the sensitivity

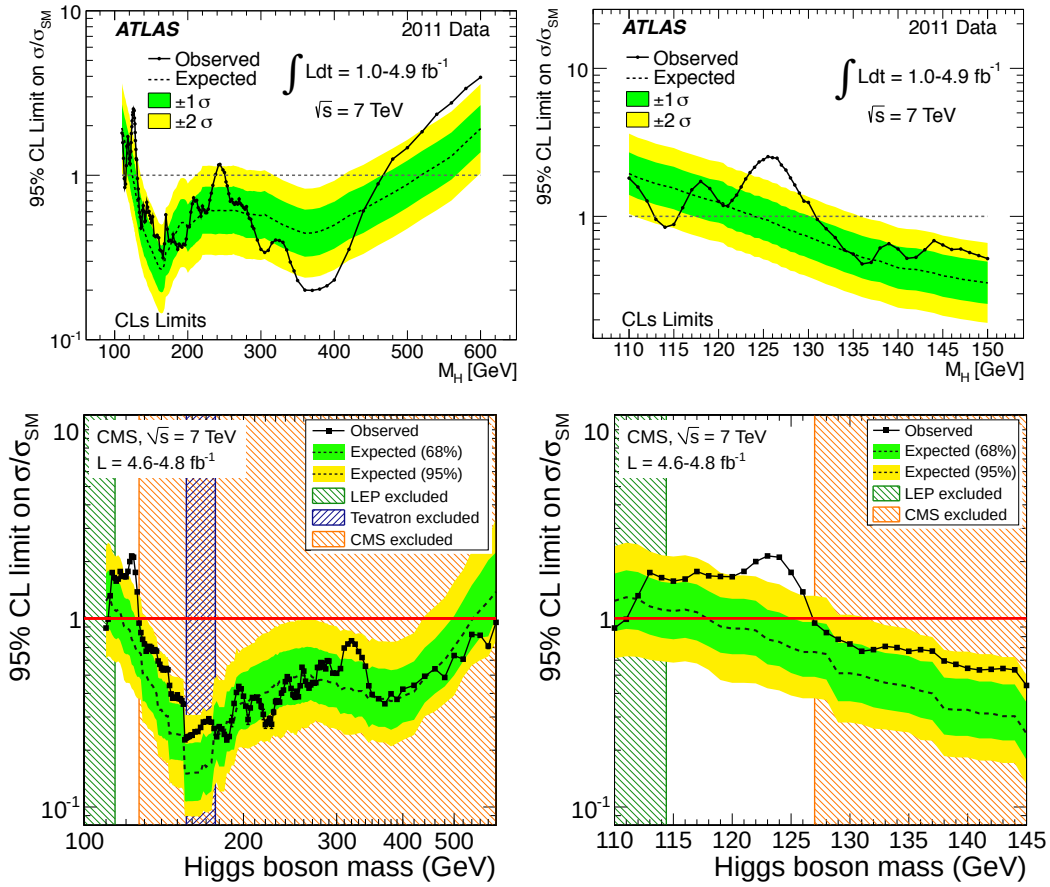

Figure 5: Upper limits from ATLAS (top) and CMS (bottom) using 2011 data with pp collisions at $\sqrt{s} = 7\,\text{TeV}$. The 95% upper limits on the signal strength parameter $\mu = \sigma/\sigma_{SM}$ for the SM Higgs boson hypothesis is plotted as function of the Higgs boson mass .

to the Higgs boson mass of precision electroweak measurements mainly at LEP, SLC, and Tevatron colliders. A global fit [23] of the results available by the summer of 2011 suggested that the Higgs boson should have a masse below 165 GeV at 95% CL. The fit gave a best mass value of $m_{\text{H}} = 91^{+30}_{-23}\,\text{GeV}$ indicating that, in the strict context of the SM, the Higgs boson should be preferably light, if it existed.

The total production cross section at the LHC is about 20 times larger than the corresponding total cross section at the Tevatron collider for $p\bar{p}$ collisions at $\sqrt{s} = 1.96\,\text{TeV}$. With about $10\,\text{fb}^{-1}$ of data collected in the D0 and CDF experiments by the end of the Tevatron lifetime, it was expected that the ATLAS and CMS experiments at the LHC would cover previous searches and take over with less than about $1\,\text{fb}^{-1}$ of data. This occurred in 2011. As for the Tevatron, the $\text{H} \to \text{WW} \to 2\ell 2\nu$ was the main channel used at the LHC for early searches of the Higgs boson. By the time of the Lepton-Photon international conference in August 2011, both LHC experiments provided an exclusion at 95% CL of the Higgs boson for masses m_{H} around $2 \times M_{\text{W}}$, in a mass window extending beyond the reach of the Tevatron experiments. From the $\text{H} \to \text{WW}$ channel alone, CMS using $1.5\,\text{fb}^{-1}$ of pp collision data at $\sqrt{s} = 7\,\text{TeV}$ excluded [24] the existence of the SM Higgs boson in the range $147 - 194\,\text{GeV}$, while ATLAS using $1.7\,\text{fb}^{-1}$ of data excluded [25] the range

$154 - 186\,\text{GeV}$.

By fall 2011, both LHC experiments had deployed first analyses in all main decay channels covering the full mass range. At higher Higgs boson masses, the search in the $H \to WW$ channel is complemented by the use of the $H \to ZZ$ channel. The $H \to WW$ decay has two modes (W^+W^- and W^-W^+). Taking into account the differences in mass between the Z and W bosons, the partial width for $H \to ZZ$ is slightly less than that of one of the WW modes, i.e. less than half of $H \to WW$. The $H \to ZZ$ nevertheless provides the best sensitivity for $M_H \gg 2 \times M_Z$ from the combination of the $H \to ZZ \to 4\ell$ and $H \to ZZ \to 2\ell 2\nu$ channels, with $\ell = e, \mu$ and $\nu = \nu_e, \nu_\mu, \nu_\tau$. These channels were combined already at the end of the 2011 data taking campaign and this lead to the rather dramatic results shown in Fig. 5. With less than $5\,\text{fb}^{-1}$ of data collected at $\sqrt{s} = 7\,\text{TeV}$ in each experiment, the full mass range for masses $m_H > 130\,\text{GeV}$ was excluded. Somehow Nature has made it as difficult as possible, possibly hiding a cherished treasure in the most inaccessible range of $114.4 < m_H < 130\,\text{GeV}$.

What followed now belongs to the history of science. Another $5\,\text{fb}^{-1}$ of data was collected at $\sqrt{s} = 8\,\text{TeV}$ until June 2012 when the experimental data was re-analysed, leading to the discovery [2, 3, 4] of a new boson around 125 GeV obtained from a combination of the di-boson channels, with leading contributions from the high resolution $H \to \gamma\gamma$ and $H \to 4\ell$ channels.

After the discovery, the landscape for the physics in relation with the Higgs boson was completely redefined. The proof of the existence of a scalar field which pervades the Universe has consequences on the history of matter, and open-up new questioning in particle physics and cosmology. Do neutrinos interact with the Higgs field? Does the Higgs boson interact with dark matter? Is there a connection between the Higgs field and the scalar field responsible for the exponential growth of the early Universe? At the LHC the research interest shifted from the search to the understanding of the exact nature of the new particle, as well as to the measurements of its properties. More than twice as much data had been collected by each of the experiments by the end of 2012. The analysis program was enriched to cover precision measurements such as its mass and width, its production cross section and quantum numbers, its couplings to other SM particles, and also searches for the rare decays such as $H \to \mu^+\mu^-$ and $H \to Z\gamma$. This was enough to confirm that the new boson has properties compatible with those expected for the Higgs boson. The analysis program has been furthermore extended to cover searches for which the Higgs boson is used as a tool to probe physics beyond the SM. The results using the full run I datasets are presented below.

5 Measurements and Properties

In the following, we review the results obtained by the ATLAS and CMS experiments for the new boson at 125 GeV, using all available data from the LHC run I. We first discuss the results obtained in individual bosonic and fermionic decay channels, and then the signal rates and coupling constraints obtained from a combination of all main channels.

5.1 High resolution decay channels and the Higgs boson mass

The mass of the Higgs boson is determined by combining two discovery channels with excellent mass resolution, namely $H \to \gamma\gamma$ and $H \to ZZ^* \to 4\ell$. In each of these channels, the instrumental mass resolution $\Delta M/M$ is expected to be in the 1-2% range. For a SM Higgs boson resonance at a mass around 125 GeV, we expect that the intrinsic width has a negligible contribution to the measured mass resolution.

The $H \to \gamma\gamma$ signal is characterized by a narrow signal mass peak over a large but smoothly falling background. The photons in background events originate from prompt non-resonant di-photon production or from jets misidentified as isolated photons. Details concerning the event selection can be found for ATLAS in Ref. [26] and for CMS in Ref. [27]. In both experiments, the analyses are split in mutually exclusive event classes to target the different production processes. The classification differ in the details between the experiments but it follow similar principles. Requiring the presence of two forward jets with high common invariant mass and

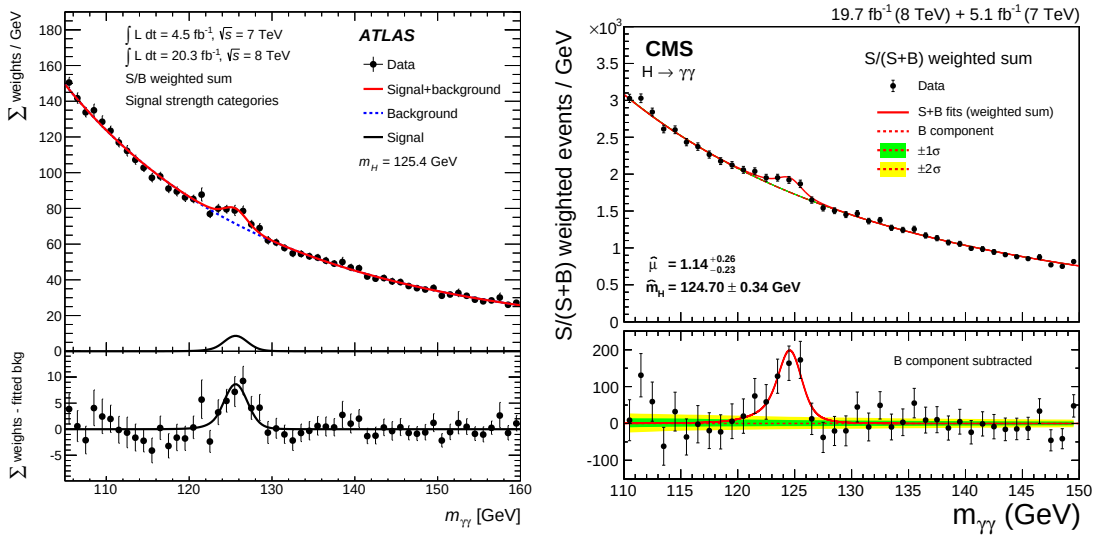

Figure 6: Distribution of the di-photon invariant mass measured in the $H \to \gamma\gamma$ analyses for run I data at 7 and 8 TeV. Combination of the event classes showing weighted data points with errors, and the result of the simultaneous fit to all categories from *(left)* ATLAS and *(right)* CMS experiments. In each case, the fitted signal plus background is shown along with the background-only component of this fit together, and the background subtracted weighted mass spectrum is shown in the bottom.

a large rapidity gap favours events produced by the VBF mechanism. Event classes designed to preferentially select VH (V = W or Z) mainly require the presence of isolated electrons, muons, or missing transverse energy E_T^{miss}, or a dijet system with an invariant mass compatible with m_W or m_Z. The remaining "untagged" events correspond mainly to the Higgs boson produced via gluon fusion and represent more than 90% of the expected signal in the SM. In both experiments, the "untagged" events are further split in categories according to the kinematics of the di-photon system, and the event-by-event estimate of the di-photon mass resolution which depends on photon reconstruction in different $|\eta|$ ranges of the detectors. In total, the ATLAS and CMS analyses rely on more than 10 categories for each of the $\sqrt{s} = 7$

and 8 TeV samples. With an unfavourable signal-to-background ratio (S/B $\ll 1$ in most categories), a key to the $H \to \gamma\gamma$ analyses is the energy calibration of photons. This is obtained by using the $Z \to ee$ candle and extrapolating to the relevant p_T range of photons, taking into account the effects from the different behaviour of photon-induced and electron-induced electromagnetic showers (e.g. shift of the longitudinal profile) in the detector. Overall, the analyses have an acceptance×efficiency of about 50% and the event categorisation is expected to improve the sensitivity by about a factor two with respect to a fully inclusive analysis. The di-photon invariant mass distribution measured by the experiments is shown in Fig. 6. A clear Higgs boson signal resonance is observed around 125 GeV. ATLAS observes [26] a signal with a local significance of 5.2σ, for a SM Higgs boson expectation of 4.6σ, at the mass obtained by the combining of the 4ℓ and 2γ channels [28]. CMS observes [27] a signal with a local significance of 5.7σ, for a SM Higgs boson expectation of 5.2σ, at the mass measured in the $\gamma\gamma$ channel in stand-alone.

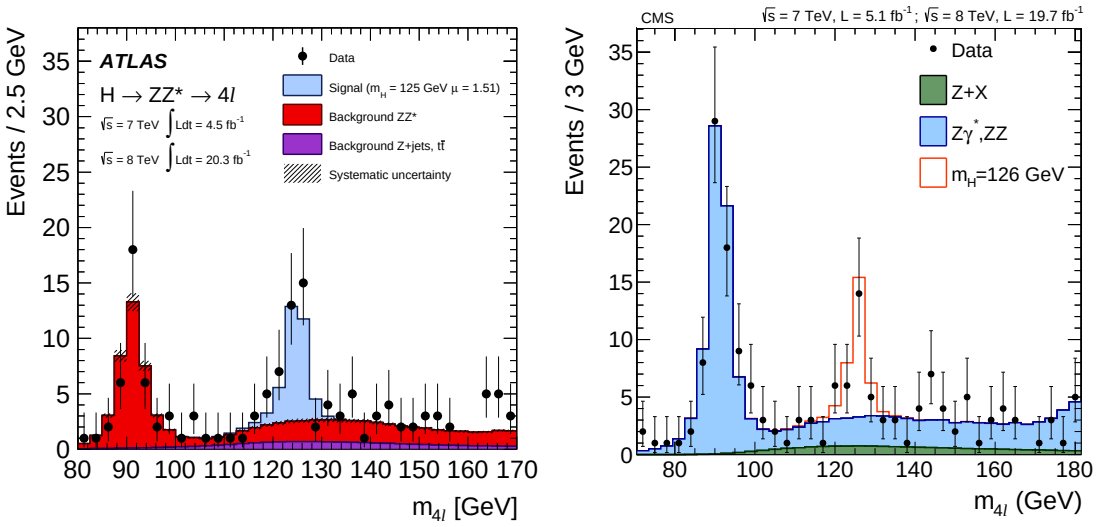

Figure 7: Distribution of the four-lepton invariant mass measured in the $H \to Z^{(*)}Z^* \to 4\ell$ analyses for run I data at 7 and 8 TeV, from *(left)* ATLAS and *(right)* CMS experiments. The plots show the sum of the $4e$, $2e2\mu$ and 4μ channels, with points with error bars representing the data, and shaded histograms representing the backgrounds. Superimposed in each case is an histogram for the Higgs boson signal expectation. This signal expectation is shown for a mass $m_H = 125$ GeV and a signal strength $\mu = \sigma_{obs.}/\sigma_{SM} = 1.51$ in the case of ATLAS, and for $m_H = 126$ GeV and the standard model expectation ($\mu = 1.00$) in the case of CMS.

The $H \to ZZ^* \to 4\ell$ signal is characterized by a narrow four-lepton ($4e, 2e2\mu$ or 4μ) mass peak over a small continuum background. Details concerning the event selection in this channel can be found for ATLAS in Ref. [29] and for CMS in Ref. [30]. The ATLAS and CMS analyses differ in the details but follow similar principles. The signal candidates are divided into mutually exclusive quadruplet categories, $4e$, $2e2\mu$ and 4μ, to better exploit the different mass resolutions and different background rates arising from jets misidentified as leptons. Four well-identified and isolated leptons are required to originate from the primary interaction vertex to suppress the Z+ jet and $t\bar{t}$ instrumental backgrounds. With a very favourable

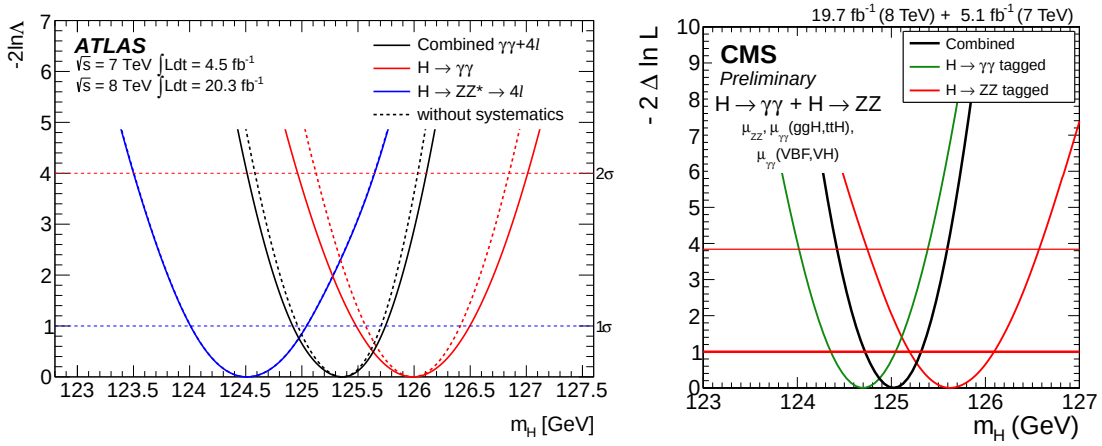

Figure 8: Scan of the likelihood test statistic versus the Higgs boson mass m_{H} for the $\mathrm{H} \to \gamma\gamma$ and the $\mathrm{H} \to 4\ell$ channels, and their combination, for *(left)* ATLAS, and *(right)* CMS.

expected signal-to-background ratio ($\mathrm{S/B} \gg 1$), a key to the $\mathrm{H} \to 4\ell$ analyses is to preserve the overall efficiency while imposing lepton identification and isolation criteria sufficient to suppress the instrumental background well below the indistinguishable background from the non-resonant ZZ continuum. The fourth lepton (i.e. with lowest p_T) has its p_T peaking well below 10 GeV for $M_{\mathrm{H}} = 125$ GeV. A high lepton reconstruction efficiency is required down to the lowest p_T consistent with the rejection of instrumental background; in practice the lowest threshold is in the range 5 to 7 GeV. The electron reconstruction makes use of rather sophisticated algorithms which combine the reconstructed track in the silicon tracker (using a gaussian sum filter technique dedicated to electrons) with clusters in the electromagnetic calorimeter, a categorization of electrons, etc. The energy scale is controlled using the $\mathrm{Z} \to \ell\ell$ candle complemented by the validation at low p_T from J/ψ and Υ(nS). The signal candidates should contain two pairs of same flavour and opposite charge leptons ($\ell^+\ell^-$ and $\ell'^+\ell'^-$). For $M_{\mathrm{H}} = 125$ GeV, the decay $\mathrm{H} \to \mathrm{Z}^{(*)}\mathrm{Z}^*$ involves at least one Z boson off mass-shell (i.e. ZZ^*), and, for about 20% of the cross section, two Z boson off mass-shell (i.e. $\mathrm{Z}^*\mathrm{Z}^*$). The analysis thus accepts a leading Z boson (Z_1) reconstructed with masses down to 40 or 50 GeV, and a subleading one (Z_2) with masses down to 12 GeV. Overall, the analyses have an acceptance×efficiency of about 20 to 40% depending on the quadruplet category. Even more sophisticated statistical analysis techniques are used beyond the baseline selection of signal candidates. In CMS, kinematic discriminants are constructed using the masses of the two di-lepton pairs and five angles, which uniquely define a four-lepton configuration in their centre-of-mass frame. These make use of leading order matrix elements for the signal and background hypothesis and are used to further separate signal and background. In ATLAS the analysis sensitivity is improved by employing a multivariate discriminant to distinguish between the Higgs boson signal from the ZZ^* background and the combination of this discriminant with the reconstructed invariant mass of the 4ℓ system is used to provide the final measurement on the Higgs boson mass in this channel.

The 4ℓ invariant mass distribution measured by the experiments is shown in

Table 2: Signal strengths and mass measurements from the high resolution di-boson channels at the LHC.

Expt.	Decay Channel	Signal Strength $\mu = \sigma_{meas.}/\sigma_{SM}$	Measured Mass (GeV) mass ± statistics ± systematics	Reference
ATLAS	H→ $\gamma\gamma$	$1.29^{+0.30}_{-0.30}$	$125.98 \pm 0.42(\text{stat}) \pm 0.28(\text{syst})$	[28]
	H→ZZ*→ 4ℓ	$1.66^{+0.45}_{-0.38}$	$124.51 \pm 0.52(\text{stat}) \pm 0.06(\text{syst})$	[28]
	Combined	—	$\mathbf{125.36 \pm 0.41}$	[28]
CMS	H→ $\gamma\gamma$	$1.14^{+0.26}_{-0.23}$	$124.7 \pm 0.31(\text{stat}) \pm 0.15(\text{syst})$	[27]
	H→ZZ*→ 4ℓ	$0.93^{+0.29}_{-0.25}$	$125.6 \pm 0.4(\text{stat}) \pm 0.2(\text{syst})$	[30]
	Combined	—	$\mathbf{125.03 \pm 0.30}$	[31]

Fig. 7. One observes a very clear Higgs boson resonance over a smooth background. The signal is observed with very high significance in both experiments. CMS observes [30] a signal with a local significance of 6.8σ, for a SM Higgs boson expectation of 6.7σ, at the mass measured in the 4ℓ channel in stand-alone. ATLAS observes [29] a signal with a local significance exceeding 8σ, for a SM Higgs boson expectation of 6.2σ, at the mass obtained by combining the 4ℓ and 2γ channels.

The measurements of the Higgs boson mass in the $\gamma\gamma$ and 4ℓ channels and for their combination are listed in Table 2, and shown in Fig. 8. These final run 1 measurements profit from the most accurate knowledge of the detector performance achieved so far, using the full datasets from proton proton collisions at the LHC in 2011 and 2012. The mass measured in the $\gamma\gamma$ channel is obtained in both experiments via a simultaneous fit of all event categories. The mass measured in the 4ℓ channel is obtained by ATLAS using a "2D" fit combining the reconstructed mass and a BDT discriminant trained on signal and ZZ* background events from Monte Carlo simulation. The mass measured in the 4ℓ channel by CMS uses a "3D" fit combining the reconstructed mass, a kinematic discriminant based on matrix elements tuned to distinguish signal from ZZ* background, and the uncertainty in the four-lepton mass estimated from detector information on a per-event basis. This is found relevant for CMS because this uncertainty varies considerably over the small number of selected signal events. In both experiments, while in the $\gamma\gamma$ channel the measurement is dominated by the systematic effects, the opposite occurs in the 4ℓ channel who suffers from low statistics. The new data taking campaign at the LHC starting in 2015 will be important to decrease the uncertainty in this measurement. A final mass value is obtained by combining the $\gamma\gamma$ and 4ℓ results. ATLAS obtains [28] a mass of $m_{\text{H}} = 125.36 \pm 0.37(\text{stat}) \pm 0.18(\text{syst})\,\text{GeV}$ (i.e. 125.36 ± 0.41). CMS obtains [31] a mass of $m_{\text{H}} = 125.03^{+0.26}_{-0.27}(\text{stat})\ ^{+0.13}_{-0.25}(\text{syst})\,\text{GeV}$ (i.e. 125.03 ± 0.30). The results are found to be consistent between channels within each experiment, and remarkably similar between the experiments for the final mass values. One notices the per-mil level of accuracy achieved in this measurement.

5.2 The Higgs boson intrinsic width

The intrinsic width (Γ_{H}) of the Higgs boson in the SM is $\Gamma_{\text{H}} \simeq 4.2\,\text{MeV}$ for $m_{\text{H}} = 125\,\text{GeV}$, corresponding to a lifetime $\tau^0_{\text{H}} = \hbar/\Gamma_{\text{H}} \simeq 2\times10^{-22}s$. This Γ_{H} is too small for a direct observation at the peak where the measured width is completely dominated by detector resolution, while at the same time too large to allow for the observation

of displaced vertices via its lifetime. At best, the experiment can verify that the lineshape at the resonance is consistent with a single narrow resonance. This has been explicitly done by both the ATLAS [26, 32] and the CMS experiments [27, 30]. ATLAS sets direct limits at 95% CL of $\Gamma_{\rm H} < 5\,\text{GeV}$ from the $\rm H \to \gamma\gamma$ channel, and $\Gamma_{\rm H} < 2.6\,\text{GeV}$ from the $\rm H \to 4\ell$ channel. CMS sets direct limits at 95% CL of $\Gamma_{\rm H} < 2.4\,\text{GeV}$ from the $\rm H \to \gamma\gamma$ channel, and $\Gamma_{\rm H} < 3.4\,\text{GeV}$ from the $\rm H \to 4\ell$ channel. A sensitivity to a range of intrinsic width values of the order of $\Gamma_{\rm H}$ is nevertheless possible by profiting from the fact that the narrow width approximation fails for the production of a Higgs boson via gluon fusion (ggH). The off-shell production cross section is sizeable and this has been exploited by the experiments in the ZZ and WW channel.

In the ZZ channel for instance, sizeable off-shell production of the Higgs boson arises from an enhancement in the decay amplitude in the vicinity of the Z-boson pair production threshold, and at higher masses from the top-quark pair production threshold. There is in addition at large mass a sizeable destructive interference with the production of a Z-boson pair from the continuum (i.e. with Z bosons coupling to quarks in a box diagram). Overall the ratio of the off-shell (above $2 \times m_{\rm Z}$) to the on-shell cross section is of the order of 8%. This sizeable contribution of the off-shell Higgs boson is not as such surprising. The Higgs boson is essential for the unitarity of the theory and it must be there to play its role in canceling the bad high energy behaviour of the continuum diagrams. The on-shell and off-shell cross section can be approximated as:

$$\sigma^{\rm on-shell}_{gg\to {\rm H}\to {\rm ZZ}^*} \approx \frac{g^2_{gg{\rm H}} g^2_{HZZ}}{m_{\rm H}\Gamma_{\rm H}} \text{ and } \sigma^{\rm off-shell}_{gg\to {\rm H}^*\to {\rm ZZ}^*} \approx \frac{g^2_{gg{\rm H}} g^2_{HZZ}}{2m_{\rm Z}} \,.$$

Thus, a measurement of the relative off-shell to on-shell signal production in the ZZ channel provides direct information on $\Gamma_{\rm H}$. Using this idea [33, 34, 35, 36], the CMS experiment has obtained [37] a constraint on the total width of $\Gamma_{\rm H} < 22\,\text{MeV}$ (i.e. 5.4 times the expected value in the SM) at 95% CL. In a similar analysis ATLAS has obtained [38] a constraint at 24 MeV (5.7 times the expected value in the SM) at 95% CL.

5.3 The Higgs boson spin-parity

Extensive tests of the spin-parity state of the new boson at the LHC have been performed in the di-boson decay channels by both the ATLAS and CMS experiments. The tests in the $\rm H \to \gamma\gamma$ channel exploit the production dependent scattering angle of the di-photon pair. In order to discriminate between the production of the resonance via $q\bar{q}$ annihilation from the production via a mixture if gg fusion and $q\bar{q}$, the experiments make use of the absolute value of the cosine of the polar angle of the di-photons in the Collins-Sopper [39] rest frame, i.e. the angle in the di-photon rest frame between the collinear photons and the line that bisects the acute angle between the colliding protons. The tests in the $\rm H \to ZZ^* \to 4\ell$ channels exploit the masses and angles reconstructed from the four leptons. The kinematic properties of the SM Higgs boson or any non-SM exotic boson decay to the four-lepton final state has been extensivly studied in the litterature (see e.g. Ref. [27] for a complete set of references), and can be described by the reconstructed masses and five production and decay angles. The tests in the $\rm H \to WW^* \to 2\ell 2\nu$ channels are production

dependent and exploit a combination of observables such as the di-lepton invariant mass $m_{\ell\ell}$, the azimuthal separation between the two leptons $\Delta\phi_{\ell\ell}$, the di-lepton transverse momentum $p_{T\ell\ell}$, and the reconstructed transverse mass m_T. ATLAS combines the sensitive observables in a BDT. CMS uses the "2D" distribution in the plane $m_{\ell\ell}$ vs. m_T, where m_T expressed in terms of the $p_{T\ell\ell}$, $\Delta\phi_{\ell\ell}$, and the missing transverse momentum in the event. In all cases, the hypothesis of a SM Higgs boson in a pure spin-parity state $J^P = 0^+$ is compared with alternative J^P hypotheses. The spin 1 is excluded in principle by the Landau-Yang theorem and the observation of the H $\rightarrow \gamma\gamma$ channel. The observation of the new boson in this channel implies that the resonance must be a boson with spin 0 or 2. Exotic spin-1 hypotheses have been nevertheless tested in the ZZ* and WW* channels. Binned likelihood fits are used to test the data for compatibility with the presence of a particle with given spin-parity J^P.

In all cases, the data is found compatible with the $J^P = 0^+$ quantum numbers of the Higgs boson, whereas alternative hypotheses are excluded with high confidence levels. The CMS results from individual di-boson channels are described in Refs.[40, 30, 27, 41]. CMS excludes $J^P = 0^-$ and $1^+, 1^-$ hypotheses at 99% CL or higher, and the spin-2 hypotheses at 95% CL or higher. The ATLAS spin-parity results for di-boson channels are described in Ref. [42]. ATLAS excludes the $J^P = 0^-, 1^+, 1^-, 2^+$ hypotheses at 97.8% CL or above. For both experiments, the exclusions are found to hold independently of the assumptions on the coupling strengths to the SM particles, and, for spin-1 and spin-2 hypothesis, of the relative fraction of gluon fusion and quark-antiquark production. Further constraints on pure and mixed spin-parity states under various assumptions have been recently established by CMS combining all di-boson channels [43]. Overall, the data thus provide strong evidence for the spin-0 nature of the Higgs boson, with positive parity being strongly preferred. The CP-even 0^+ hypothesis is found to be favoured over any other pure spin-parity state hypothesis at a level of more than 3 standard deviations.

5.4 The fermionic decay modes and non-universality

The H$\rightarrow b\bar{b}$ decay channel is studied in the VH production mode with V = W or Z, and with V undergoing leptonic decays [44, 45]. Final states with 2 b jets from the H decay, and with zero, one, or two charged leptons (electrons or muons) from the V decays are considered by the experiments, targeting Z$\rightarrow \nu\nu$, W$\rightarrow e\nu, \mu\nu$, and Z$\rightarrow ee, \mu\mu$ respectively. The channel W$\rightarrow \tau\nu$ is also considered in CMS in the case where the τ decay involves one charged hadron, i.e. the so-called "single-prong" decays. The key elements of the analysis are to obtain a high efficiency in tagging the b-jets, a low rate of misidentified jets as b-jets, and an estimation of the backgrounds from the data. Requirements on the missing transverse energy and/or on the azimuthal opening angle between the missing transverse momentum and the direction of the b jets (or of the leptons) are imposed. To further improve on the sensitivity, the analysis for each final state is further divided in categories according to the p_T boost of the H or the V bosons. The H and the V bosons recoil against each other and a substantial reduction of the background can be achieved in high p_T boost kinematic regions [46]. For the statistical analysis of the selected events, ATLAS employs a binned likelihood constructed as the product of distributions for the invariant mass $m_{b\bar{b}}$ in 26 signal regions, while CMS employs a combination of 14 boosted-decision tree (BDT) discriminants. While signal over background (S/B)

ratios in the range of 0.1% to 1.0% are expected when integrating around the signal peak at $m_{b\bar{b}} \simeq 125\,\text{GeV}$, this improves up to about 10% for events with highest BDT scores. The $t\bar{t}$ production is among the main backgrounds in all event categories. It dominates the event yield in the signal region for WH production after the full event selection. The V+$b\bar{b}$ production is the dominating background for ZH production.

The H$\rightarrow \tau^+\tau^-$ decay channel is studied in the ggH, VBF, and VH production modes [47, 48], with $\tau_\ell\tau_\ell, \tau_\ell\tau_h$ and $\tau_h\tau_h$ in the final state, where $\tau_\ell = \tau_e$ or τ_μ designates tau leptons decaying leptonically, and τ_h designates tau leptons decaying semi-leptonically (with one or more charged hadrons in the final state). To enhance the sensitivity in the ggH or VBH production modes, the events are classified in categories according to the number of additional jets and to kinematic quantities that exhibit differences for the signal and background events. Categories with large p_T (boosted) reconstructed Higgs boson enhance the sensitivity to ggH production. Categories with 2 high p_T jets separated by a large rapidity gap target VBF production. CMS also considers VH production, requiring one or two additional leptons (electrons or muons) compatible with a leptonic decay of the W or Z boson. For the statistical analysis of the selected events, ATLAS uses a combination of BDTs, built in the various $\tau_\ell\tau_\ell, \tau_\ell\tau_h$ and $\tau_h\tau_h$ channels from a set of discriminating variables, to combine the VBF and boosted exclusive categories. CMS employs a likelihood product with the signal extracted in the different channels from the distribution of the invariant mass of the tau lepton pair, except in the WH and in the ee and $e\mu$ channels where kinematics discriminants are used. Signal over background (S/B) ratios or the order of 10% are achieved in the three bins with highest BDT score, and reaches S/B$\simeq$1 for the VBF bin with highest BDT score of ATLAS (as for the "tight VBF category" of CMS) where 10-20 signal events are expected.

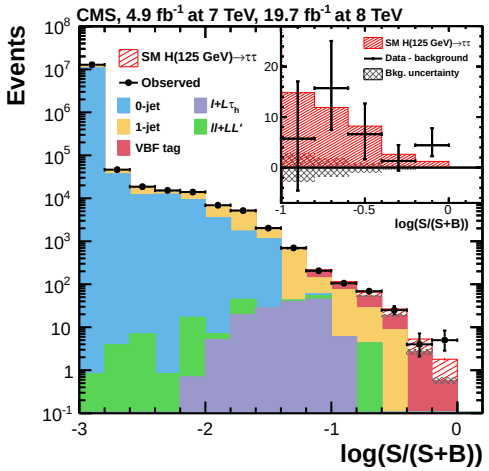

Figure 9: Combined observed and predicted distributions for the H$\rightarrow \tau^+\tau^-$ observations by the CMS experiment [48]. Similar results are obtained by the ATLAS experiment [47]. The results are presented grouped in bins of the $\log(S/S+B)$ for the final discriminators used for the various event categories, with $(S/S+B)$ denoting the ratio of the predicted signal (S) and signal-plus-background ($S+B$) event yields in each bin.

In the H$\rightarrow b\bar{b}$ channel, ATLAS observes [44] a 1.4σ excess with respect to the background only hypothesis, for an expectation of 2.6σ for the SM Higgs boson. CMS observes [45] an excess of 2.1σ compared to an expectation for the SM Higgs boson of 2.1σ. The statistics in the VH production mode is too small at the LHC to establish at this stage a direct evidence for H$\rightarrow bb$. The most significant evidence so far for H$\rightarrow bb$ comes from the CDF and D0 experiments at the Tevatron. Combining their analyses in the VH production modes, the Tevatron experiments [49, 50] find

an excess of signal candidates with a significance of 2.8σ at the LHC mass $m_{\mathrm{H}} = 125\,\mathrm{GeV}$, and a maximum local significance of 3.3σ at 135 GeV.

In the $\mathrm{H}\to\tau^+\tau^-$ channel, both LHC experiments find clear evidence for a Higgs boson signal [47, 48], thus establishing, beyond the knowledge available at the time of the discovery, the first evidence that the Higgs boson couples to leptons. CMS finds [45] a 3.4σ excess with respect to the background only hypothesis, for an expectation of 3.6σ for the SM Higgs boson. The observations in the various event categories used for the analysis are illustrated in Fig. 9. A combination of the $b\bar{b}$ and $\tau^+\tau^-$ decay channels [51] yields an evidence for the coupling to these fermions at 3.8σ (4.4σ expected). In the $\mathrm{H}\to\tau^+\tau^-$ channel, ATLAS finds [44] a 4.1σ excess for an expectation of 3.2σ for the SM Higgs boson. The evidence for the $\mathrm{H}\tau\tau$ coupling combined with the null evidence so far for the $\mathrm{H}\mu\mu$ coupling [52, 53] implies that the new boson has non-universal family couplings. The scalar sector could play an important role in the origin of fermion families.

5.5 Combined measurements of signal rates and couplings

A coherent statistical analysis of the full set of analysis channels allows to slightly improve the measurements of the signal rates for individual production and decay modes of the Higgs boson, as well as to establish a coherent set of constraints on the Higgs boson couplings to different particle species.

For the measurement of signal rates, the inputs to the combined analyses are in principle the experimental results obtained in individual, i.e. "stand-alone" and mutually exclusive analyses discussed in previous sections of this paper. In practice, the ATLAS and CMS combinations make use of more or different information, and uses the information from individual channels in a different manner. At this stage, this is partly because only preliminary combination results are available. ATLAS first published in summer 2013 a combination of di-boson channels using all available run I data [29], but the results in individual decay channels have been since then superseded in some cases. A new combination of the five main decays channels and preliminary results in individual channels is now available [54], but this one does not yet include for instance the latest $\mathrm{H}\to\gamma\gamma$ from ATLAS [26]. CMS first published final sets of results using all available run I data in each of the main five decays channels, and presented a preliminary combination in summer 2014 [31] which incorporate additional information analysis targeting specific production modes such as $t\bar{t}\mathrm{H}$ [55]. Also, the combination profits from new theory information in some areas. For instance, since the publication of the stand-alone analysis, the search for VH production with $\mathrm{H}\to\mathrm{b\bar{b}}$ decays has been improved for CMS [31] by the use of recent NLO calculations for the gluon fusion loop contribution to ZH production. The organization of the information also differ for some individual decay channels. For CMS the input to the combination is organized in terms of decay "tags". For instance the $\mathrm{H}\to\tau\tau$ "tag" includes some signal contamination from $\mathrm{H}\to\mathrm{WW}^*$, etc. The signal strengths for such decay "tags" which serve as inputs to the combination in CMS cannot be interpreted literally as compatibility tests for pure production mechanisms or decay modes, in contrast to the results from the stand-alone analysis.

The $\gamma\gamma$, ZZ, and WW di-boson channels were the main contributors to the original discovery and have been exploited for the determination of the Higgs boson mass, intrinsic width, and spin-parity state. For the combination, both the ATLAS and CMS experiment assume a single CP even scalar state (0^+) resonance with a mass

obtained by the combination of the H → γγ and H → ZZ* → 4ℓ (ℓ = e, μ) channels, as established from the di-boson decay channels discussed in previous sections. While the mass of the Higgs boson is a free parameter in the SM, the number of Higgs bosons events decaying in each channel is quite accurately predicted by theory; thus measuring the ratio μ between the number of observed events over the number of predicted events (signal strength) we have an easy way to test the consistency with the SM ($\mu = 1$ means that what we observe is the SM Higgs boson). To obtain specific constraints on the Higgs boson couplings, a simultaneous analysis of all production and decay channels is necessary to account in consistent manner for all all statistical uncertainties, systematic certainties, and their correlations. Furthermore, the production×decay for the Higgs boson at the LHC is always sensitive to a combination, linear at LO, of two couplings. Thus some model assumptions are required to disentangle the effects of each coupling. This is done following the prescription of the LHC Cross Section Working group. A narrow width approximation such that $\sigma \times \beta_i = \sigma_i \times \Gamma_i/\Gamma_{\rm H}$ is considered and SM "kappa" modifiers are introduced for the production, $\kappa_i^2 = \sigma_i/\sigma_i^{\rm SM}$, and decay $\kappa_j^2 = \Gamma_j/\Gamma_i^{\rm SM}$, with $\kappa_{\rm H} = (\sum \kappa_j^2 \Gamma_j^{\rm SM})/\Gamma_{\rm H}^{\rm SM}$. Various benchmark scenarios are then studied [54, 31].

The signal strength μ measured in various decay channels by ATLAS [54] and CMS [31] experiments is shown in Fig. 10. In both experiments, all signal strengths

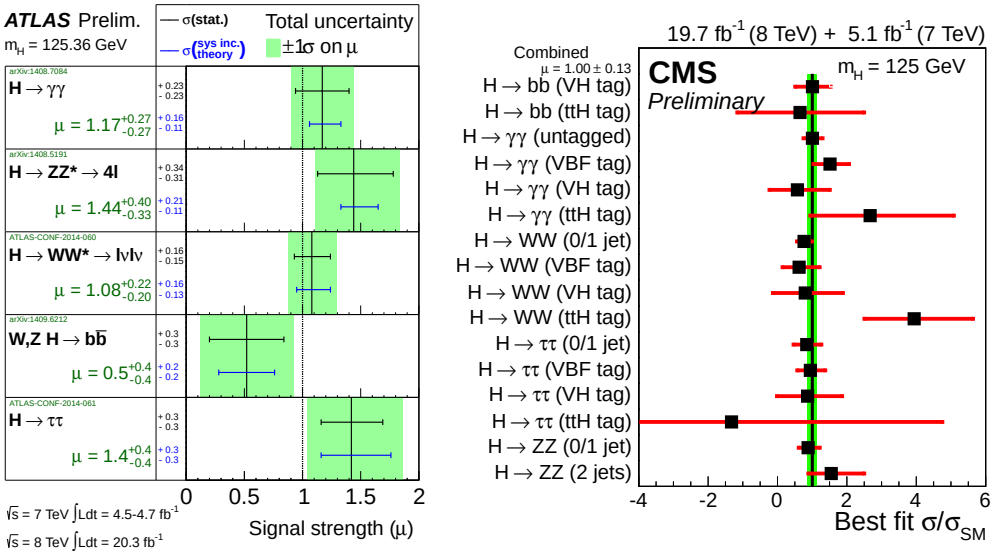

Figure 10: The signal strength μ at the measured Higgs boson masses by the *(left)* ATLAS and *(right)* CMS experiments. For ATLAS the best-fit values are shown by the solid vertical lines with ± 1 standard deviation uncertainties indicated by green shaded bands, and the contributions from statistical uncertainty (top), the total (experimental and theoretical) systematic uncertainty (bottom) indicated within the bands. For CMS, the best fit value for the combination is shown as a solid vertical line and the overall uncertainty as a vertical band; the points are the results from sub-combinations by predominant decay mode or production mode tag. The uncertainties include both statistical and systematic uncertainties.

measured are consistent with the expectation for the Higgs boson in the SM within one to two standard deviations. The best fit signal strengths μ for di-bosons measured in ATLAS are seen in Fig. 10 (left) to be slightly above expectations, with

1.17 ± 0.27 ($H \to \gamma\gamma$), $1.44^{+0.40}_{-0.33}$ ($H \to ZZ^*$), $1.08^{+0.22}_{-0.20}$ ($H \to WW^*$). A signal strength of 1.4 ± 0.4 is obtained for $H \to \tau\tau$. A value of 0.5 ± 0.4 is obtained for $H \to b\bar{b}$. Combining all all five main decay channels, using their previous $H \to \gamma\gamma$ result [29], ATLAS finds $\mu = 1.30 \pm 0.12(stat)^{+0.14}_{-0.11}(syst)$. The Fig. 10 (right) show the signal strengths in the various "tags" from CMS. The signal strengths μ combining the various "tags" obtained for each of the 5 main decay channel tags are 1.13 ± 0.24 ($H \to \gamma\gamma$), 1.00 ± 0.29 ($H \to ZZ^*$), 0.83 ± 0.21 ($H \to WW^*$), 0.91 ± 0.27 ($H \to \tau\tau$), and 0.93 ± 0.49 ($H \to b\bar{b}$). Combining all five main decay channels, CMS finds $\mu = 1.00 \pm 0.13$. The top quark is involved in virtual loops for the ggH production, the main production channel at the LHC, as well as in virtual loops for $H \to \gamma\gamma$ decay where it interferes with loops involving the W boson. Indirect evidence for the Higgs boson coupling to the top quark is thus obtained. The other heavy fermions of the third generation, the b quark and the τ lepton, are involved in the dominating Higgs boson decay modes. Evidence has been found for the $H \to \tau\tau$ decay as was discussed in previous sections. The bottom quark is involved mainly in the decay $H \to b\bar{b}$ where only a small excess of events has been observed so far.

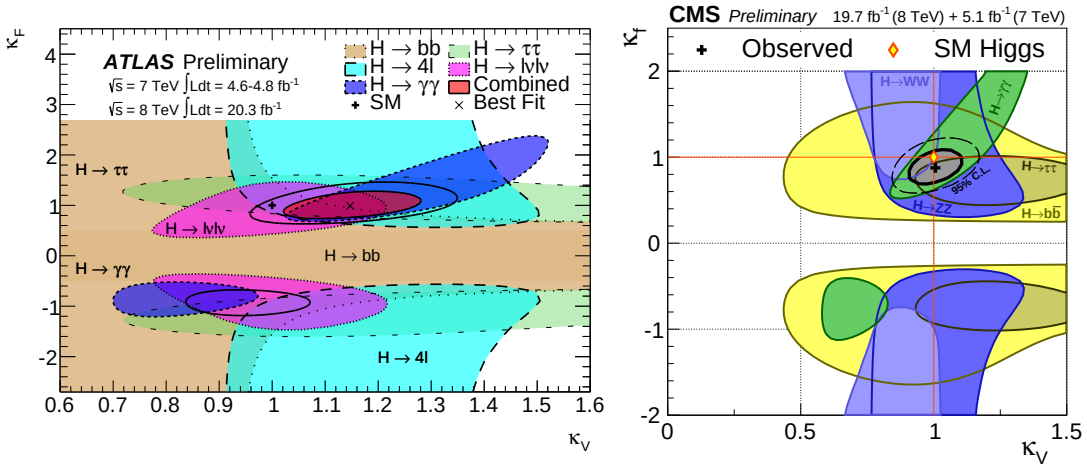

Figure 11: The 68% contours for individual decay channels (bounded colored regions) and for the overall combination (thick curves) in the correlation plane (κ_V, κ_F), the coupling scale factors for bosons (κ_V) and fermions (κ_F), from *(left)* ATLAS and *(right)* CMS. The standard model expectation is indicated at $(\kappa_V, \kappa_F) = (1, 1)$. The likelihood scans are shown in the two quadrants, assuming either like signs $(+, +)$ or unlike signs $(+, -)$.

The data from different decay channels can be associated to different production "tags" as was shown for example in Fig. 10 (right). Each production mechanism can be in turn associated to either fermion couplings (ggH, $t\bar{t}$H) or to vector-boson couplings (VBF, VH). From the combined fit, the signal strength for the VH and VBF production can be assessed. An evidence is obtained for the observation of VBF production with a significance of 4.1σ for ATLAS [29, 54], and 3.7σ for CMS [31]. For the VH production, CMS observes a significance of 2.7σ for an expectation of 2.9σ [31].

The ATLAS and CMS constraints on the Higgs boson coupling to fermions

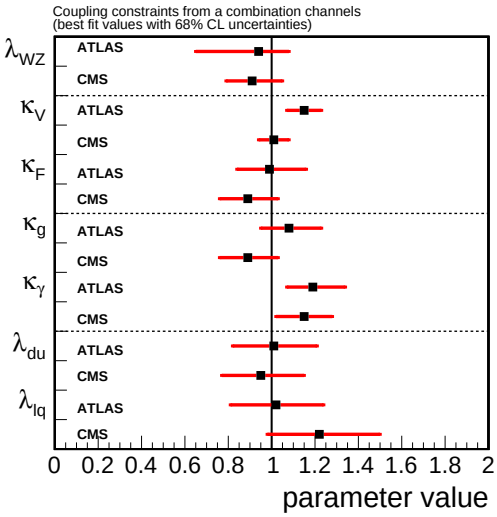

Figure 12: Summary of the "best fit" values obtained for different fits to the full set of Higgs boson analysis channels.

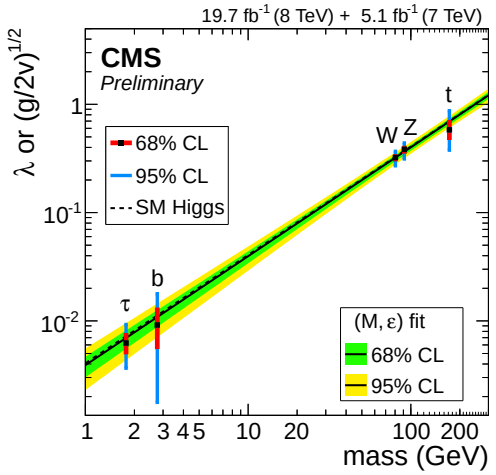

Figure 13: Summary of the "best fit" values obtained for different particle species, and expressed as function of the known particle mass. The results are shown for illustration here from CMS [31]. Similar results are obtained by ATLAS [54]. For the fermions, the values of the fitted Yukawa couplings Hff are shown. For the vector bosons, the square-root of the coupling for the HVV vertex, divided by two times the vacuum expectation value of the Higgs boson field are shown.

$(\kappa_F = \kappa_\ell = \kappa_q)$ and electroweak bosons $(\kappa_V = \kappa_{\rm W} = \kappa_{\rm Z})$ are shown in Fig. 11. The data are compatible with the expectation for the SM Higgs boson: the SM point of $(\kappa_V, \kappa_F) = (1, 1)$ is within the 95%CL contour for ATLAS, and within the 68%CL contour for CMS. The fits in Fig. 11 are shown allowing for opposite signs of the κ_V and κ_F. The sensitivity to this relative sign comes from the negative interference between the loop contributions involving either W bosons or top quarks in the $\rm H \to \gamma\gamma$ decay. In other words, at LO $\Gamma_{\gamma\gamma}$ involves a product $\kappa_W \kappa_t$ while all other partial decay widths scale as κ_V^2 or κ_F^2. The $(\kappa_V, \kappa_F) = (1, -1)$ is found to be disfavoured at the $\sim 2\sigma$ level by ATLAS results, and at the $\sim 3\sigma$ level by CMS results.

The combined data has been used to further test the compatibility of the observations with the SM Higgs boson couplings, by fitting to a subset of coupling modifiers. In the SM, the custodial symmetry fixes the relative couplings $\lambda_{\rm WZ} = \kappa_{\rm W}/\kappa_Z$ of the Higgs boson to W and Z bosons to $\lambda_{\rm WZ} = 1.0$. ATLAS obtains a best fit for this ratio of $0.94^{+0.14}_{-0.29}$ while CMS obtains $0.91^{+0.14}_{-0.12}$. From a fit for the couplings to bosons κ_V and and fermions as free parameters, ATLAS obtains a best fit of $(\kappa_V, \kappa_F) = (1.15^{+0.08}_{-0.08}, 0.99^{+0.17}_{-0.15})$ while CMS obtains $(\kappa_V, \kappa_F) = (1.01^{+0.07}_{-0.07}, 0.89^{+0.14}_{-0.13})$. For the effective couplings to gluons κ_g and photons κ_γ as free parameters, AT-

LAS obtains best fit values of $\kappa_g = 1.08^{+0.15}_{-0.13}$ and $\kappa_\gamma = 1.19^{+0.15}_{-0.12}$, while CMS obtain $\kappa_g = 0.89^{+0.10}_{-0.10}$ and $\kappa_\gamma = 1.15^{+0.13}_{-0.13}$. Fits allowing for a different ratio of the couplings to down-type and up-type fermions ($\lambda_{du} = \kappa_d/\kappa_u$) or, separately, for a different ratio of the couplings to leptons and quarks ($\lambda_{\ell q} = \kappa_\ell/\kappa_q$) have been performed. These fits are motivated by theories beyond the standard model (BSM) where the couplings to different type of fermions can be modified, such in supersymmetric models. CMS obtains $\lambda_{du} = 1.01^{+0.20}_{-0.19}$ and $\lambda_{\ell q} = 1.02^{+0.22}_{-0.21}$. ATLAS obtains $\lambda_{du} = 0.95^{+0.20}_{-0.18}$ and $\lambda_{\ell q} = 1.22^{+0.28}_{-0.24}$ around the SM-like minima. All coupling results are consistent with the expectation for the SM Higgs boson. These results are collected for convenience in Fig. 12. The Fig. 13 illustrate the results from the best fit values for the couplings for different particle species. The couplings are found to scale with mass as expected for a Higgs boson of the BEH mechanism. Finally, constraints can be obtained on possible BSM contributions by allowing for a non-vanishing partial width into invisible or undetected particles. Upper limits at 95% CL for the branching ratio into such BSM particles of 41% and 58% are obtained by ATLAS and CMS respectively.

6 Conclusions and the Aftermath

The boson discovered in 2012 at the LHC by the ATLAS and CMS experiments has properties consistent, within uncertainties, with the Higgs boson of the standard model. The analysis of the full sets of data collected during run I at the LHC at 7 and 8 TeV has allowed for considerable progress in the characterization of this H boson. Having determined the Higgs boson mass m_{H} with a relative precision $\Delta m/m$ well below the per-mil level, all the production and decay properties of a H boson are predicted by the theory and can be compared with data. The custodial symmetry is verified to $\sim 15\%$. The relative couplings of the H boson with d-like and u-like quarks of the third generation is verified at the $\sim 30\%$ level. The couplings to fermions of the third generation is verified at the $\sim 15 - 20\%$ level. Overall, the couplings to boson and fermions are verified to $\sim 15\%$ and consistent with the SM expectation at the $\sim 1\sigma$ level, and, thus, scale as expected as a function of the fermion and vector boson masses. The existence of a boson with non-universal family couplings is established via the evidence for $\mathrm{H} \to \tau\tau$ and the null evidence for $\mathrm{H} \to \mu\mu$. More data will be needed to further disentangle the various production and decay modes, and provide more stringent constraints on the couplings.

The existence of a scalar field and the spontaneous electroweak symmetry breaking mechanism, provide an explanation for the origin of the Z and W and ordinary fermion masses and solves, or postpones to much higher energy, the problem of the unitarization of the theory. As a consequence, stringent constraints are established for global fits in the electroweak sector by injecting the H boson mass in the global fit of precision electroweak data: The W boson is predicted with a precision better than that of direct measurements. The discovery marks the triumph of the weak couplings in the history of matter in the universe; a culmination of a reductionism strategy which has evolved from questions of the structure of matter to questions on the very origin of interactions (local gauge symmetries) and matter (interactions with Higgs field). An important aspect of the theory nevertheless remains to be constrained by the experiments, namely the coupling of the Higgs field with itself. This self-coupling is at the origin of the so-called "condensation" of the Higgs field which is expected to drive the EWSB mechanism. The shape of the scalar

potential for the Higgs field that is responsible for EWSB depends on m_{H} and on the trilinear and quadrilinear self-couplings. In the SM, these are presumed to be fundamentally related. The trilinear coupling for the physical Higgs boson which enters for instance in di-H production is given in the SM by $\lambda_{\mathrm{HHH}} = 3m_{\mathrm{H}}^2/v$, where $v = (\sqrt{2}G_F)^{-1/2} \approx 246\,\mathrm{GeV}$ is the mean vacuum expectation value for the Higgs field. The observation of the di-H production and extraction of constraints on λ_{HHH} is one the menu for the high luminosity runs at the LHC during the next five years, and a measurement is reachable at very high luminosity with a future upgraded LHC collider.

Besides the mass, spin-parity, and couplings of the Higgs boson, there still remain the questions of the origin and stabilization of its mass at the weak scale. This question of a "natural" stabilization of the Higgs boson mass had been a central incentive for the developments of theories beyond the standard model (BSM) for many decades. In so-called "Technicolor" theories, one assumes that the SM is only an effective theory which breaks up at the TeV scale where a new strong interaction sets in. In so-called "extra dimension" theories, the validity of the SM is assumed to be limited at the TeV scale where strong effects of quantum gravity propagating in all dimensions would set in. Supersymmetric theories offer in principle a more satisfactory solution in the scalar sector. The self-coupling can possibly be expressed in a combination of gauge couplings in such theories such that the scalar sector is strongly constrained, e.g. with a predicted mass for the lightest, possibly SM-like, neutral Higgs boson. The stabilization of the Higgs scalar boson is obtained, despite the introduction of the new scale for the breaking of the supersymmetry, by exact cancellations of the contributions of the new supersymmetric particles, the partners of ordinary fermions and bosons.

In the years to come, the LHC collider with operate at higher instantaneous luminosities, and higher pp centre-of-mass energies. The aim is to reach $300\,\mathrm{fb}^{-1}$ of integrated luminosity at $\sqrt{s} = 13\,\mathrm{TeV}$ in a first phase, and then $3000\,\mathrm{fb}^{-1}$ at $\sqrt{s} = 14\,\mathrm{TeV}$ in a second phase. These forthcoming data taking periods could allow for the observation of deviations from expectation or for the direct discovery of extra structure in the scalar sector, beyond the minimal sector of the standard model.

Acknowledgments

I wish to thank my colleagues from the ATLAS and CMS collaborations for their support in preparing this review. Thanks to Olivier Davignon and Roberto Salerno from the CMS group at the Laboratoire Leprince-Ringuet for comments and suggestions. This review borrows and extends from a previous review that I prepared on behalf of ATLAS and CMS experiments for the "25th Rencontres de Blois" in 2013, as well as for a more recent review in preparation with Rosy Nicolaidou from the IRFU, CEA-Saclay, for the "Comptes Rendues de l'Académie des Sciences". The results summarized here have been made possible thanks to the very successful operation of the LHC by the CERN accelerator departments. Thanks above all to colleagues from the technical and administrative staffs at CERN and at other ATLAS and CMS institutes for their contributions to the success of the experiments at the LHC.

References

[1] Particle Data Group, K. Nakamura et al., *Review of particle physics*, J. Phys. **G37** (2010) 075021.

[2] ATLAS Collaboration, G. Aad et al., *Observation of a new particle in the search for the Standard Model Higgs boson with the ATLAS detector at the LHC*, Phys. Lett. **B716** (2012) 1–29, arXiv:1207.7214 [hep-ex].

[3] CMS Collaboration, S. Chatrchyan et al., *Observation of a new boson at a mass of 125 GeV with the CMS experiment at the LHC*, Phys. Lett. **B716** (2012) 30–61, arXiv:1207.7235 [hep-ex].

[4] CMS Collaboration, S. Chatrchyan et al., *Observation of a new boson with mass near 125 GeV in pp collisions at $\sqrt{s}$ = 7 and 8 TeV*, JHEP **1306** (2013) 081, arXiv:1303.4571 [hep-ex].

[5] S. Glashow, *Partial Symmetries of Weak Interactions*, Nucl. Phys. **22** (1961) 579–588.

[6] S. Weinberg, *A Model of Leptons*, Phys. Rev. Lett. **19** (1967) 1264–1266.

[7] A. Salam, *Weak and Electromagnetic Interactions*, Proceedings of the eighth Nobel symposium - N. Svartholm, ed. **C680519** (1968) 367–377.

[8] F. Englert and R. Brout, *Broken Symmetry and the Mass of Gauge Vector Mesons*, Phys. Rev. Lett. **13** (1964) 321–323.

[9] P. W. Higgs, *Broken symmetries, massless particles and gauge fields*, Phys. Lett. **12** (1964) 132–133.

[10] P. W. Higgs, *Broken Symmetries and the Masses of Gauge Bosons*, Phys. Rev. Lett. **13** (1964) 508–509.

[11] G. Guralnik, C. Hagen, and T. Kibble, *Global Conservation Laws and Massless Particles*, Phys. Rev. Lett. **13** (1964) 585–587.

[12] P. W. Higgs, *Spontaneous Symmetry Breakdown without Massless Bosons*, Phys. Rev. **145** (1966) 1156–1163.

[13] T. Kibble, *Symmetry breaking in nonAbelian gauge theories*, Phys. Rev. **155** (1967) 1554–1561.

[14] J. M. Cornwall, D. N. Levin, and G. Tiktopoulos, *Uniqueness of spontaneously broken gauge theories*, Phys. Rev. Lett. **30** (1973) 1268–1270.

[15] J. M. Cornwall, D. N. Levin, and G. Tiktopoulos, *Derivation of Gauge Invariance from High-Energy Unitarity Bounds on the s Matrix*, Phys. Rev. **D10** (1974) 1145.

[16] C. Llewellyn Smith, *High-Energy Behavior and Gauge Symmetry*, Phys. Lett. **B46** (1973) 233–236.

[17] B. W. Lee, C. Quigg, and H. Thacker, *Weak Interactions at Very High-Energies: The Role of the Higgs Boson Mass*, Phys. Rev. **D16** (1977) 1519.

[18] ATLAS Collaboration, G. Aad et al., *The ATLAS Experiment at the CERN Large Hadron Collider*, JINST **3** (2008) S08003.

[19] CMS Collaboration, S. Chatrchyan et al., *The CMS experiment at the CERN LHC*, JINST **3** (2008) S08004.

[20] LHC Higgs Cross Section Working Group, S. Heinemeyer et al., *Handbook of LHC Higgs Cross Sections: 3. Higgs Properties*, arXiv:1307.1347 [hep-ph].

[21] LEP Working Group for Higgs boson searches, ALEPH Collaboration, DELPHI Collaboration, L3 Collaboration, OPAL Collaboration , R. Barate et al., *Search for the standard model Higgs boson at LEP*, Phys. Lett. **B565** (2003) 61–75, arXiv:hep-ex/0306033 [hep-ex].

[22] TEVNPH Working Group, CDF Collaboration, D0 Collaboration , *Combined CDF and D0 Searches for the Standard Model Higgs Boson Decaying to Two Photons with up to 8.2 fb^{-1}*, arXiv:1107.4960 [hep-ex].

[23] M. Baak, M. Goebel, J. Haller, A. Hoecker, D. Ludwig, et al., *Updated Status of the Global Electroweak Fit and Constraints on New Physics*, Eur. Phys. J. **C72** (2012) 2003, arXiv:1107.0975 [hep-ph].

[24] CMS Collaboration, *Search for the Higgs Boson in the Fully Leptonic W^+W^- Final State*, CMS-PAS-HIG-11-014, http://cds.cern.ch/record/1376638.

[25] ATLAS Collaboration, *Search for the Standard Model Higgs boson in the $H \to WW^{(*)} \to \ell\nu\ell\nu$ decay mode ...* , ATLAS-CONF-2011-134, http://cds.cern.ch/record/1383837.

[26] ATLAS Collaboration, G. Aad et al., *Measurement of Higgs boson production in the diphoton decay channel in pp collisions at center-of-mass energies of 7 and 8 TeV with the ATLAS detector*, arXiv:1408.7084 [hep-ex].

[27] CMS Collaboration, V. Khachatryan et al., *Observation of the diphoton decay of the Higgs boson and measurement of its properties*, arXiv:1407.0558 [hep-ex].

[28] ATLAS Collaboration, G. Aad et al., *Measurement of the Higgs boson mass from the $H \to \gamma\gamma$ and $H \to ZZ^* \to 4\ell$ channels with the ATLAS detector using 25 fb^{-1} of pp collision data*, arXiv:1406.3827 [hep-ex].

[29] ATLAS Collaboration, G. Aad et al., *Measurements of Higgs boson production and couplings in diboson final states with the ATLAS detector at the LHC*, Phys. Lett. **B726** (2013) 88–119, arXiv:1307.1427 [hep-ex].

[30] CMS Collaboration, S. Chatrchyan et al., *Measurement of the properties of a Higgs boson in the four-lepton final state*, Phys. Rev. **D89** (2014) 092007, arXiv:1312.5353 [hep-ex].

[31] CMS Collaboration, *Precise determination of the mass of the Higgs boson and studies of the compatibility of its couplings with the standard model*, CMS-PAS-HIG-14-009, http://cds.cern.ch/record/1728249.

[32] ATLAS Collaboration, G. Aad et al., *Measurements of Higgs boson production and couplings in the four-lepton channel in pp collisions at center-of-mass energies of 7 and 8 TeV with the ATLAS detector*, arXiv:1408.5191 [hep-ex].

[33] F. Caola and K. Melnikov, *Constraining the Higgs boson width with ZZ production at the LHC*, Phys. Rev. **D88** (2013) 054024, arXiv:1307.4935 [hep-ph].

[34] N. Kauer and G. Passarino, *Inadequacy of zero-width approximation for a light Higgs boson signal*, JHEP **1208** (2012) 116, arXiv:1206.4803 [hep-ph].

[35] N. Kauer, *Inadequacy of zero-width approximation for a light Higgs boson signal*, Mod. Phys. Lett. **A28** (2013) 1330015, arXiv:1305.2092 [hep-ph].

[36] J. M. Campbell, R. K. Ellis, and C. Williams, *Bounding the Higgs width at the LHC using full analytic results for* $gg \to e^- e^+ \mu^- \mu^+$, JHEP **1404** (2014) 060, arXiv:1311.3589 [hep-ph].

[37] CMS Collaboration, V. Khachatryan et al., *Constraints on the Higgs boson width from off-shell production and decay to Z-boson pairs*, Phys. Lett. **B736** (2014) 64, arXiv:1405.3455 [hep-ex].

[38] ATLAS Collaboration, *Determination of the off-shell Higgs boson signal strength in the high-mass ZZ final state with the ATLAS detector*, ATLAS-CONF-2014-042, http://cds.cern.ch/record/1740973.

[39] J. C. Collins and D. E. Soper, *Angular Distribution of Dileptons in High-Energy Hadron Collisions*, Phys. Rev. **D16** (1977) 2219.

[40] CMS Collaboration, S. Chatrchyan et al., *Study of the Mass and Spin-Parity of the Higgs Boson Candidate Via Its Decays to Z Boson Pairs*, Phys. Rev. Lett. **110** (2013) 081803, arXiv:1212.6639 [hep-ex].

[41] CMS Collaboration, S. Chatrchyan et al., *Measurement of Higgs boson production and properties in the WW decay channel with leptonic final states*, JHEP **1401** (2014) 096, arXiv:1312.1129 [hep-ex].

[42] ATLAS Collaboration, G. Aad et al., *Evidence for the spin-0 nature of the Higgs boson using ATLAS data*, Phys. Lett. **B726** (2013) 120–144, arXiv:1307.1432 [hep-ex].

[43] CMS Collaboration, *Constraints on the spin-parity and anomalous HVV interactions of the Higgs boson from the CMS experiment*, CMS-PAS-HIG-14-018, http://cds.cern.ch/record/1969386.

[44] ATLAS Collaboration, G. Aad et al., *Search for the* $b\bar{b}$ *decay of the Standard Model Higgs boson in associated* $(W/Z)H$ *production with the ATLAS detector*, arXiv:1409.6212 [hep-ex].

[45] CMS Collaboration, S. Chatrchyan et al., *Search for the standard model Higgs boson produced in association with a W or a Z boson and decaying to bottom quarks*, Phys. Rev. **D89** (2014) 012003, arXiv:1310.3687 [hep-ex].

[46] J. M. Butterworth, A. R. Davison, M. Rubin, and G. P. Salam, *Jet substructure as a new Higgs search channel at the LHC*, Phys. Rev. Lett. **100** (2008) 242001, arXiv:0802.2470 [hep-ph].

[47] ATLAS Collaboration, *Evidence for Higgs Boson Decays to the $\tau^+\tau^-$ Final State with the ATLAS Detector*, ATLAS-CONF-2013-108, http://cds.cern.ch/record/1632191.

[48] CMS Collaboration, S. Chatrchyan et al., *Evidence for the 125 GeV Higgs boson decaying to a pair of τ leptons*, JHEP **1405** (2014) 104, arXiv:1401.5041 [hep-ex].

[49] CDF Collaboration, D0 Collaboration, T. Aaltonen et al., *Evidence for a particle produced in association with weak bosons and decaying to a bottom-antibottom quark pair in Higgs boson searches at the Tevatron*, Phys. Rev. Lett. **109** (2012) 071804, arXiv:1207.6436 [hep-ex].

[50] CDF Collaboration, D0 Collaboration, T. Aaltonen et al., *Higgs Boson Studies at the Tevatron*, Phys. Rev. **D88** (2013) no. 5, 052014, arXiv:1303.6346 [hep-ex].

[51] CMS Collaboration, S. Chatrchyan et al., *Evidence for the direct decay of the 125 GeV Higgs boson to fermions*, Nature Phys. **10** (2014) , arXiv:1401.6527 [hep-ex].

[52] ATLAS Collaboration, G. Aad et al., *Search for the Standard Model Higgs boson decay to $\mu^+\mu^-$ with the ATLAS detector*, Phys. Lett. **B738** (2014) 68–86, arXiv:1406.7663 [hep-ex].

[53] CMS Collaboration, V. Khachatryan et al., *Search for a standard model-like Higgs boson in the $\mu^+\mu^-$ and e^+e^- decay channels at the LHC*, arXiv:1410.6679 [hep-ex].

[54] ATLAS Collaboration, *Updated coupling measurements of the Higgs boson with the ATLAS detector using up to 25 fb^{-1} of proton-proton collision data*, ATLAS-CONF-2014-009, https://cds.cern.ch/record/1670012.

[55] CMS Collaboration, V. Khachatryan et al., *Search for the associated production of the Higgs boson with a top-quark pair*, JHEP **1409** (2014) 087, arXiv:1408.1682 [hep-ex].